EFFECT OF MACHINING ON DAMAGE AND STRENGTH OF GREEN CERAMICS

A Thesis
Presented to
The Academic Faculty

by

Jesse P. Castellana

In Partial Fulfillment
of the Requirements for the Degree
Master of Science in the
School of Mechanical Engineering

Georgia Institute of Technology
May 2021

EFFECT OF MACHINING ON DAMAGE AND STRENGTH OF GREEN CERAMICS

Approved by:

Dr. Shreyes Melkote, Advisor
School of Mechanical Engineering
Georgia Institute of Technology

Dr. Christopher Saldana
School of Mechanical Engineering
Georgia Institute of Technology

Dr. Steven Liang
School of Mechanical Engineering
Georgia Institute of Technology

Date Approved: [April 28, 2021]

ACKNOWLEDGEMENTS

There are many people who deserve thanks for ensuring that I could complete this thesis. First is my advisor, Dr. Melkote, who has guided me through this process and supplied unending encouragement and feedback. Thanks also go to Dr. Liang and Dr. Saldana for taking the time and effort to be members of my reading committee.

I would like to thank the people at Corning Inc. for funding this project, providing ceramic samples, and for guiding me through this project. Mr. Steven Sheffield and the rest of the staff at the Montgomery Machining Mall assisted in setting and up using the lathe. Dr. James Collins from the Material Properties and Characterization Facility helped setup the Instron machine used in the bending experiments. Vinh Nguyen as well as my other colleagues in the Precision Machining Research Consortium deserve thanks for training me on various devices necessary for these experiments. Finally, I would like to thank my parents for their support.

TABLE OF CONTENTS

LIST OF TABLES

LIST OF FIGURES

LIST OF SYMBOLS AND ABBREVIATIONS

MC	Methyl-cellulose
HMC	Hydroxypropyl-methyl-cellulose
PCD	Polycrystalline diamond
ANOVA	Analysis of variance
PCC	Polymer coagulation casting
$\boldsymbol{\sigma_0}$	Weibull characteristic strength
m	Weibull shape parameter
Alumina	Aluminum oxide (Al_2O_3)

SUMMARY

Powder ceramics are being used in new applications including car engine valves and dental implants. These ceramics are formed by mixing ceramic particles with polymer binders into a slurry and then either casting, extruding, or pressing them into a shape. They are then dried and fired. Various methods exist for shaping and post-processing the ceramics after firing. However, these techniques often suffer from high cost or low efficiency. An alternative is to machine the ceramics before firing, while they are in what is called the green state. This is much cheaper and has higher material removal rates than machining in the fired state.

Machining of fired ceramics is known to induce damage that reduces the strength of the machined part. Green machining has also been shown to reduce strength. However, the mechanism for this reduction and how aspects of machining and the material composition impact the magnitude of the reduction is unclear. This thesis examines the relationship between machining parameters and material composition on resultant forces and surface roughness in green turning of aluminum oxide rods. The effect of force and roughness on the strength is also studied.

The first set of experiments involved turning green alumina samples at various levels of the machining parameters and for samples made with different material compositions to understand how these factors impacted the resultant force and surface roughness. A design of experiment was used and the results showed that feed and rake angle were important for both forces and roughness, and that particle size was important for forces. Other factors and their second level interactions were also statistically

significant, but the above factors had the largest effects. It is notable that higher feed led to lower resultant force. This may be because ploughing rather than cutting occurred at low feeds, resulting in higher forces. Additionally, cutting with a positive rake angle tool resulted in higher force than with a neutral rake angle tool.

For the second round of experiments, longer alumina rods were turned on a lathe and then tested in four-point bending test for strength in the green state. A subset of the machining and material factors from the first round of experiments were varied during turning to achieve different resultant forces and surface roughness. The forces and roughness were then correlated with bending strength. The results showed that neither force nor roughness had a statistically significant effect on strength. This indicates that either the machining induced damage, if any occurred, is minor compared to the internal flaws from extrusion or that the reduction in strength is minor compared to the inherent variability of strength between green samples. Another possibility is that machining induced damage is less important in the more ductile green state than in the brittle fired state. Future work should focus on understanding how green machining impacts fired strength.

.

CHAPTER 1. INTRODUCTION

1.1 Background

Powder ceramics products are manufactured by extruding a ceramic powder with a polymer binder to hold the particles together into a fixed shape. The extruded ceramic is then dried and fired, at which point the ceramic becomes harder and more brittle.

Different machining methods can be used on the fired ceramic to achieve the final shape and dimensions. This includes mechanical material removal techniques such as diamond grinding, ultrasonic machining, polishing, and lapping, as well as electrical, chemical, and laser machining techniques. Many of these methods suffer from high cost, and some have low machining accuracy or low process efficiency [1]. Diamond grinding is one of the more common techniques for shaping sintered ceramics, but it suffers from the above issues. In addition, many of these methods are not efficient for achieving complex shapes for the final part. Traditional machining of sintered ceramics can result in complex shapes, but this has been shown to cause subsurface damage that can reduce strength [2]. Films, coatings, or polishing can be used to compensate for the damage, but this adds to the overall cost [3].

A powder ceramic is in the green, or unfired, state when it has just been dried but not yet sintered. At this stage, the ceramic is soft enough that traditional machining techniques such as turning and milling can be utilized to reach final dimensions and shape before firing. This process is known as green machining, and it can achieve complex shapes more efficiently than fired grinding. Because the ceramic is softer in the green state, green

machining can reach higher material removal rates, increasing process efficiency and reducing cost.

1.2 Motivation

Application of powder ceramics is limited by the ability to machine the fired parts into complex shapes. Fired powder ceramics are traditionally shaped with diamond grinding, which is expensive and inefficient for hard ceramics. Alternatively, the extrusion die can be sized to extrude a blank close to the desired final shape and dimensions, minimizing the amount of machining necessary post-firing. However, dies are limited in the shapes they can extrude and custom dies for complex shapes are expensive. Machining the ceramics in the green state can achieve more complex shape and do so more efficiently than diamond grinding.

Despite its advantages, green machining is not widely used and limited research has been done to understand the cutting process with green ceramics. Additionally, the brittle nature of powder ceramics ensures that any cracks will lead to premature failure under normal operating loads. Minimizing the size and frequency of surface defects formed during green machining is important for part reliability. However, it is not well understood how the cutting forces and surface roughness produced during green machining impact the strength of the green part. In addition, the way that process parameters during machining and the material composition of the green part impact aspects of machining such as cutting force and surface roughness has also not been studied sufficiently. Process parameters during machining and characteristics of the powder ceramic and binder have been shown in limited cases to impact the forces and surface roughness of the green parts [4-13]. A

more comprehensive investigation that examines these factors together is needed to fully understand the reduction in bending strength from green machining. Once the impact of green machining on bending strength is better understood, recommendations can be made for improving the strength of the final powder ceramics, thus increasing their usability.

1.3 Research Objectives

The goal of this thesis to understand the nature of strength reduction as a result of machining induced damage in green alumina ceramics and how it relates to machining process parameters, material characteristics of the green ceramic, cutting forces, and surface roughness.

The specific research objectives are:

1. Determine the impact of process parameters and green alumina characteristics on cutting forces and surface roughness during turning.
2. Relate the reduction in bending strength from machining induced damage to the cutting forces and surface roughness.

1.4 Approach

The research goals are achieved through experimental methods using fractional factorial designs to determine the effects of input factors on output measurements. Two sequential investigations are conducted with the first identifying factors that determine the magnitude of the cutting forces during machining and the resulting surface roughness of the machined surfaces. The second investigation focuses on the narrower subset of factors

by using them to produce samples of varying cutting forces and surface roughness to determine how those two characteristics relate to the bending strength of the green ceramic.

The first round of experiments involves turning small sections of green alumina rods and measuring the machining forces. Afterwards, the machined sections are evaluated for surface roughness and surface morphology. Factors including the process parameters such as the feed, cutting speed, and rake angle and the constituents and composition of the green ceramic are varied between tests to determine their impact on the above measurements.

The second round of experiments involves turning longer sections of the green alumina rods and repeating the same measurements as in the first investigation. A subset of the factors examined in the first experiments are again varied in this round of experiments. In addition, the green ceramic rods are measured for bending strength to determine the extent of strength reduction from machining induced damage.

1.5 Thesis Outline

This thesis is organized into the following four chapters. Chapter 2 reviews the literature on machining green ceramics, especially those relating to machining induced damage and the effect of process parameters or material characteristics on the cutting process. The first round of experiments are explained in detail in Chapter 3. Analysis is provided with a discussion of which factors should be included in the follow-up experiments. Those follow-up experiments are then described and analyzed in Chapter 4. Finally, Chapter 5 discusses the results of both sets of experiments, draws conclusions, and makes recommendations for future work.

CHAPTER 2. LITERATURE REVIEW

2.1 Introduction

This chapter reviews the literature on green machining of ceramics. Much work has been done to find methods of producing green bodies with high enough strength for machining in the green state. This is important because green ceramics often don't have high enough strength to be clamped or machined without fracturing spontaneously, or sustaining severe damage. Machining studies often examine the machinability and surface roughness of green parts as a factor of the process parameters during machining and the material characteristics of the green ceramic. Little work has studied cutting forces in green machining or how those forces affect strength.

The effect of process parameters on cutting force and surface roughness in green ceramics is well understood, but the effect of material characteristics only partially. This is problematic given the many processes used for producing green parts, the different binders and additives used, and the relative proportion of each ingredient. This is often because many material factors are connected. Changing the level of one factor affects another, so studying them in isolation is difficult.

Experiments have been performed looking at the strength of both unfired and fired parts after green machining. Some of these results are contradictory and more clarity is needed if parts are to have high enough strength post-machining.

2.2 Producing Green Ceramics

Various methods are used to form green ceramics. The first uses isostatic pressing to form a green blank from ceramic particles and polymer binder [7, 14, 15]. However, pressed ceramics often have gradients in their particle density, which can cause warpage during sintering. Green machining is often needed to remove those sections with gradients before sintering [9, 13]. Another method is gelcasting, where ceramic particles are mixed with monomers in a slurry, before being polymerized in a mold with a crosslinking agent [9]. Next is polymer coagulation casting (PCC), which uses water soluble proteins as the binder [8, 12, 16]. A catalyst is added to the mold, breaking the hydrogen bonds of the protein and causing the chains to uncoil and form agglomerates. Last is gelforming, which is similar to gelcasting, except that a polymer binder that has already been crosslinked is used instead of a monomer binder, and that extrusion is used instead of a mold. This method often uses higher content of the binder, but is difficult to use for large parts because of long drying times [16].

2.3 Surface Roughness

Material characteristics of the green ceramic are known to affect surface roughness after green machining. In particular, the different processes for forming the green parts can impact roughness. Gelforming was shown to create smoother surfaces than gelcasting and PCC [12, 16]. Figure 1 shows the machined surfaces for samples made with the three techniques. It was speculated that this may be because of the higher binder content used in gelforming. However a separate study on gelcast green ceramics showed that roughness increased with binder content when grinding [4].

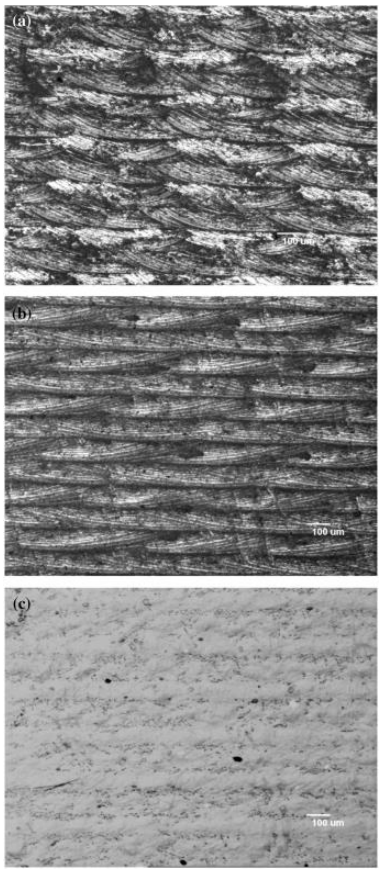

Figure 1 - Machined surfaces of alumina made with three different processes. From top to bottom, they are PCC, gelcasting, and gelforming [12].

Additionally, the process parameters of each method can impact roughness. For example, the ratio of monomer to crosslinking agent in gelcasting can change the surface roughness [9]. Material characteristics also often interact in their effect on surface roughness. One study showed that adding wax and nano-scale ceramic powders to a slurry changed the roughness and that the two additives interacted in their effect. However, this was not separated from the effect of particle size, shape, and binder content [11].

The impact of process parameters during green machining on surface roughness is much clearer. Higher feed is known to increase roughness in green turning and milling,

and feed is often the most important factor in determining roughness. Cutting speed, however, has no effect [7, 11].

Lastly, sintering the green ceramic has been shown to improve the surface roughness [8]. If roughness is an important determinant of strength in the fired state, then this implies that sintering may partially undo strength reduction from green machining.

2.4 Machining Force

Only a small number of studies have examined cutting forces in green machining. In green grinding experiments, forces were lower for samples with a lower binder content [4]. Additionally, a micro-planing study found that the presence of wax in the binder of a green ceramic reduced forces because it reduced the interlocking of the particles [10]. A follow up study with micro-milling showed that the interaction of wax and the addition of nano-particle ceramics had a significant effect on forces [11]. However, the effects of these factors are confounded by uncontrolled factors, including the size of the particles, their shape, and the overall binder content. In particular, binder content was already shown to be important for cutting forces in the grinding experiments [4].

Forces in various green machining operations have been shown to depend on the process parameters. In green grinding, larger depth of cut was found to increase forces [4]. Turning experiments have shown that higher feed and depth of cut increase forces, as seen in Figure 2 [7]. Higher feed and cutting speed have been shown to increase forces in micro-machining, but feed had a much larger effect than speed [10, 11]. Interestingly, increasing the feed in samples with the wax removed led to lower forces. This is believed to be due to more cutting than ploughing occurring at the higher feed [10]. In micro-machining, the

edge radius of the tool was important when the uncut chip thickness was on the same order of magnitude as the edge radius. A smaller edge radius generated lower force and relatively more cutting than ploughing in orthogonal cutting conditions. Lastly, greater hardness of the green part and increased wear of the tool may also increase forces [11].

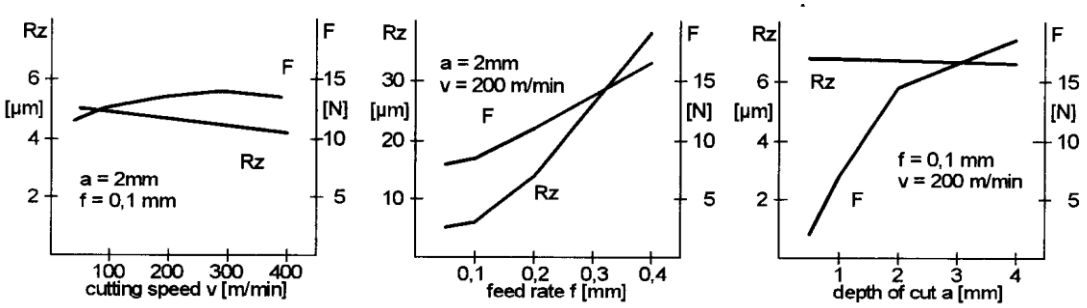

Figure 2 - Data from turning of pressed alumina. Cutting speed, feed, and depth of cut are plotted against force and roughness [7].

2.5 Strength and Machining Induced Damage

Investigations into strength have looked at how aspects of the forming process impact the green strength. Additionally, the effects of process parameters during green machining and the material characteristics of the green ceramic on strength in the green and fired states have been examined.

Comparisons of different green forming processes show that gelforming resulted in stronger blanks than PCC, and that gelcasting was stronger than isostatic pressing. Additionally, the ratio of monomer to crosslinking agent was important for the strength of gelcast parts [9, 12].

Material characteristics of the green blank have been studied for their effect on strength after machining. Higher binder content in pressed AlN was shown to increase the

green strength after machining. Additionally, using a thermoset polymer as the binder was found to increase strength over a thermoplastic because the binder distributed itself more homogenously among the ceramic particles [5]. Some evidence shows that smaller particle size for the ceramic powder increases strength because the diameter of the pores are smaller. However, this is confounded with the packing density, solid loading, the phase of the ceramic, and binder content [6].

Research into the effect of process parameters on strength have mainly focused on the impact of feed because feed has been shown to increase surface roughness in green machining, as discussed previously [7, 11]. Since brittle ceramics fail from the largest flaw, a rougher surface from high feed machining could reduce strength. Tests have been conducted to determine how green machining impacts the strength before and after sintering.

In one study using Weibull statistics for strength, higher feed during green machining was found to have no effect on the characteristic strength of alumina samples evaluated in the green state, and that the Weibull modulus actually increased from higher feed. When tested in the fired state, higher feed reduced both the strength and modulus [7]. Another study reported the same results for green machined alumina samples tested in the green state, but the opposite when they were tested in the fired state: higher feed increased the strength and the modulus [13]. Comparisons of green machined samples with polished samples found that machining reduced strength in the fired state [8, 12]. Overall, the effect of green machining on strength is not clear due to contradictory evidence.

The mechanism for strength reduction after machining is believed to be through damage done to the surface. One study described two mechanisms of material removal when green machining. The first is cutting of the granules, which are agglomerates of the ceramic powder particles and the binder. This cutting mode is characterized by feed marks on the machined surface. The second mechanism involves spalling the granules out of the workpiece, leaving craters on the surface. This second mechanism was argued to cause damage through surface roughening [7]. One study argued that these cutting modes were connected to transgranular and intergranular fracture respectively. SEM images were used to show that transgranular fracture cut the granules, leaving a cleaved surface, while intergranular fracture left intact granules on the surface, as seen in Figure 3 [5].

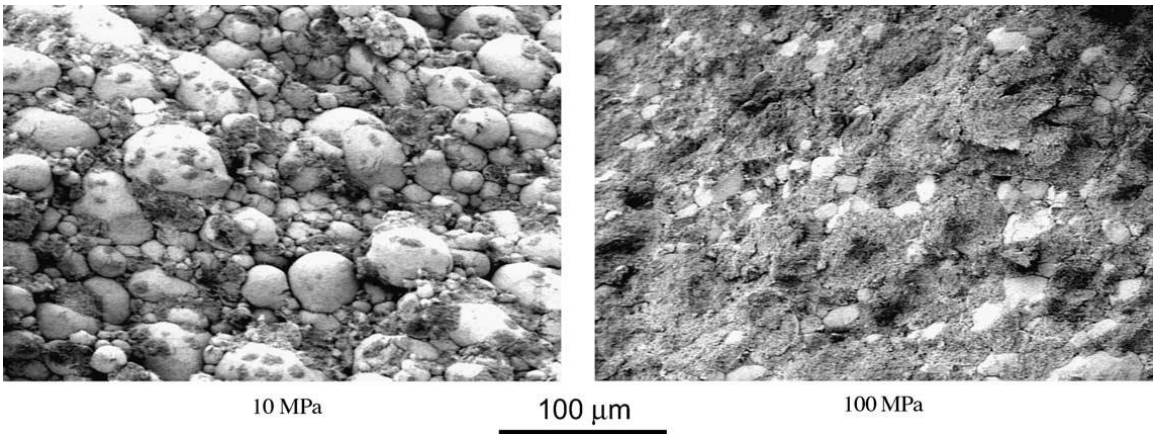

Figure 3 - Fractured surfaces of dry pressed aluminum nitride that were pressed with different pressures. The left image shows intergranular fracture and the right show transgranular fracture. [5].

Another study used an FEA analysis to determine how process parameters in orthogonal cutting impacted the size of cracks on the surface after green machining. It was shown that the tool rake angle was the most important factor by far, with a more negative

rake angle reducing crack size. The feed and cutting speed were found to have a much smaller effect, with lower feed and higher speed reducing the crack size [15].

2.6 Tool Wear

Because green ceramics consist of abrasive particles, tool wear is often severe in green machining. Wear has been noted for machining with high speed steel, tungsten carbide, and cermet tools [4, 5, 11, 16]. Tool wear varies among different varieties of ceramic particles, and some evidence suggests it varies with hardness. Excessive tool wear may also lead to higher forces in cutting [11]. Therefore, diamond coated tools are recommended and have been used in green machining successfully [16].

2.7 Discussion

Much is still not known about how the material composition of the green ceramic impacts the forces and roughness during machining. Because it is difficult to change the level of one factor without also changing another factor, the effect of many material factors are confounded with each other in multiple studies. Material composition factors need to be studied for their individual effect and for their interactions with each other as well as their interactions with machining parameters. In addition, the effect of rake angle has only been studied in numerical simulations, and only for its effect on surface cracks, not for cutting forces or surface roughness.

Strength reduction after green machining is not well understood, and the effect of cutting forces on strength has not been directly examined. Some studies have tried to show that surface roughness was the determining factor for green strength after machining, but

this is contradicted by other studies. A more systematic examination of the relationship between cutting force and surface roughness on strength after green machining is necessary to determine how the strength reduction can be minimized for practical application of green machining.

CHAPTER 3. EFFECT OF CUTTING PARAMETERS AND MATERIAL COMPOSITION

3.1 Introduction

The goal of this thesis is to understand how green machining impacts the strength of the green ceramic parts. Machining is assumed to impact the strength through the cutting forces and surface roughness. Chapter 4 explores that linkage. Before that, however, it must be understood how both cutting force and roughness are impacted by process parameters during machining and material characteristics of the green ceramic.

The first round of experiments was performed to determine how those factors impact the cutting forces during turning and the roughness of the machined surfaces. Longitudinal turning was performed on short lengths of the unfired alumina rods in a lathe. Forces were measured by a piezoelectric cutting force dynamometer attached to the cutting tool, and the surface roughness of the machined sections were measured with a white light scanning interferometer. A design of experiments was used to vary the process and material related factors across cutting tests so that statistical analysis could be performed for the correlations between those factors and the measurements.

3.2 Experimental Procedure

3.2.1 Ceramic Rods

All of the unfired aluminum oxide (Al_2O_3, alumina) rods used in these experiments were produced by Corning Incorporated. These rods were created by first mixing the dry

ingredients in a powder blender/mixer (Turbula). The dry ingredients include alpha alumina powder, modified smectite clay, and colloidal bohemite. Then the cellulose binder was added to the dry mixture in a standard kitchen blender. A Brabender plasticizer was then used to plasticize the new mixture. Next, the mixture was placed in an extruder where it de-aired for 10 minutes before being extruded through a 19.05 mm (0.75") die. The extruded rods were finally dried in a humidity controlled dessicator using a 3A molecular sieve. The percentages by volume of these ingredients are listed in Table 1.

Table 1 - Volume percent of ingredients in green alumina rods.

	Cellulose	**Alpha Alumina Powder**	**Colloidal Bohemite**	**Modified Smectite Clay**
% Volume	3	88	10	2

The final dimensions of the extruded rods were 95.25 mm (3.75") long by 19.05 mm (0.75") diameter. Four different batches of rods were produced each using one of two cellulose binders and one of two sizes of alumina particles. The two binders were methyl-cellulose (MC) and hydroxypropyl-methyl-cellulose (HMC), while the alumina particles came in fine and coarse ground sizes. One batch was produced for each combination of the two parameters. Table 2 shows the batch names for the four combinations. Another four batches were also created using a smaller percent volume of binder, but these were too brittle for machining, and would spontaneously fracture under even gentle machining conditions. Therefore, only the four batches listed in Table 2 were used in the experiments.

Table 2 - Batch names of alumina rods split by combination of particle size and cellulose binder type.

	Fine	Coarse
MC	BB3	BB7
HMC	BB1	BB5

3.2.2 Experimental Setup

The cutting experiments were performed on an Okuma Spaceturn LB2000 CNC lathe. The lathe uses a pneumatic chuck to clamp samples, but the minimum clamping pressure would crush the brittle alumina rods if they were inserted directly. Instead, the rods were placed in a cylindrical aluminum collar, with three set screws on the periphery tightened to hold the rods in place. The collar could then be placed in the chuck without the rods being crushed.

Forces were measured by a Kistler 9256C2 dynamometer, bolted onto one of the lathe's turrets. The cutting tool was affixed to the dynamometer with a custom fixture. Additionally, the inside of the lathe was covered with plastic drop cloth so that the abrasive alumina particles could not get between moving parts and cause damage. A vacuum cleaner with a HEPA filter was also pointed towards the cutting edge to collect alumina particles. Figure 4 shows the full setup.

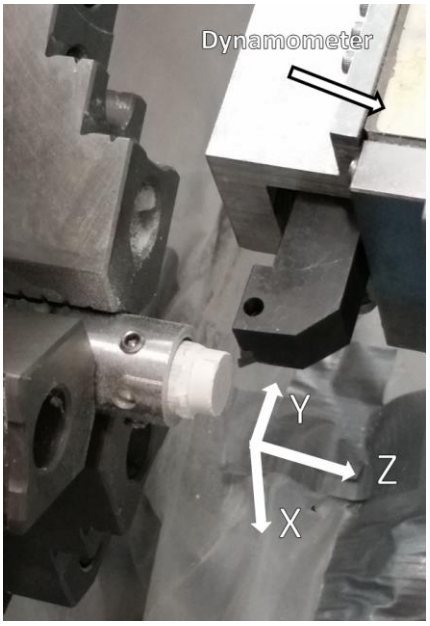

Figure 4 - Experimental setup for longitudinal turning, with the dynamometer and its coordinate system labeled.

The dynamometer collects force data in three orthogonal directions using the coordinate system shown in Figure 4. Data from the dynamometer goes through a charge amplifier (Kistler 5010B) before being read by a data acquisition card (National Instruments 9232). Raw data files are then produced using the Labview program, which are imported into MATLAB for analysis.

A start and end point was chosen for the region where steady state force was observed. The data between those points were averaged in each direction. Equation 1 shows that the average resultant force, F_R, was calculated with the average steady state forces in each direction: F_X, F_Y, and F_Z. Figure 5 shows a representative force profile for one direction with the steady state region marked.

The raw force signal oscillates with a pattern that repeats once per revolution of the spindle due to deflection of the green part. For example, the data shown in Figure 5 is from

a test using 75 m/min linear cutting speed and a sample with a diameter of 14.5 mm. The equivalent spindle speed to achieve that cutting speed is 1646.43 rev/min, which is equivalent to a period of 0.036 seconds. That is approximately the period for the oscillations in Figure 5. Other cutting tests with different spindle speeds also had oscillations whose period matched one revolution of the spindle. Averaging is used to reduce the oscillating force signal to a single value.

$$F_R = \sqrt{F_X^2 + F_y^2 + F_Z^2} \tag{1}$$

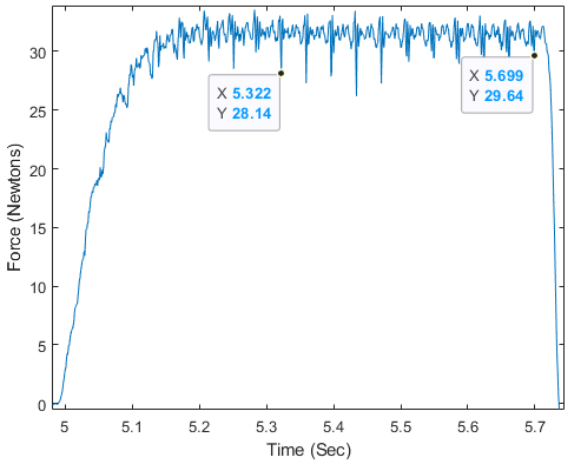

Figure 5 - Raw force signal in the y-direction. Start and end points for the steady state region are marked. Sample was made with HMC binder and coarse particle size. Turning used 0.25 mm/rev feed, 75 m/min speed, and a zero degree rake tool.

Extruded rods have an oval cross-section and an outer skin. Before cutting experiments can be performed, the outer diameter of the rods are reduced on the lathe until the skin is removed and the rod is a straight cylinder. Preliminary tests showed that cutting with different lengths of the rod sticking out from the collar resulted in higher forces for cuts performed closer to the chuck face. To control for this, only 10.16 mm (0.4") length

of rod was allowed to protrude from the collar for each test. Additionally, all of the cutting tests used 5.08 mm (0.2”) length and had 2.54 mm (0.1”) radial depth of cut.

3.2.3 Imaging

After each test, the machined section was removed using a diamond wire saw (Murg 24-A) with low feed to avoid further damaging the rod. The machined surface was then examined using a ZeGage Pro white light scanning interferometer. The interferometer measures a square section of the machined surface and calculates the arithmetic average deviation of the three dimensional roughness, or Sa. The software for the profilometer, MX, also corrects for the curvature of the machined surface. Five measurements were taken for each cutting test and averaged. Lastly, a Leica DVM6 optical microscope was used to take images of the machined surface of each cut section.

3.2.4 Experimental Design

Table 3 shows the experimental testing matrix for this round of experiments. The matrix uses a 2^{5-1} half fractional factorial design. This gives a resolution of five, which ensures that main effects and secondary effects of each factor are clear. Sixteen treatment combinations were used with five repetitions for each, resulting in 80 total data points.

Five factors are varied between two levels. The first three are process parameters for turning, including the feed, the cutting speed, and the rake angle of the cutting edge. Feed and speed were included because they have been shown to impact force and roughness [7, 11]. Rake angle was also added because finite element simulations have shown that it is important for surface cracking [15]. The other two are material

characteristics of the unfired alumina rod, including the type of cellulose binder and the size of the alumina particles used in the extruded rods. The type of binder was used as a factor because different binders can change the mode of fracture and impact the strength [5]. Lastly, particle size has been shown to impact green strength, but only in a study where it was confounded with other factors [6].

Table 3 - Experimental test matrix for longitudinal cutting experiments.

Treatment	Feed	Cutting Speed	Rake Angle	Cellulose	Particle Size
1	-	-	-	-	+
2	-	-	-	+	-
3	-	-	+	-	-
4	-	-	+	+	+
5	-	+	-	-	-
6	-	+	-	+	+
7	-	+	+	-	+
8	-	+	+	+	-
9	+	-	-	-	-
10	+	-	-	+	+
11	+	-	+	-	+
12	+	-	+	+	-
13	+	+	-	-	+
14	+	+	-	+	-
15	+	+	+	-	-
16	+	+	+	+	+

The low and high levels for each factor are shown in Table 4. The particular values for feed and cutting speed were chosen after preliminary cutting tests. Values from another green turning study were used as a starting point [7]. These tests found that the green ceramics often failed spontaneously during cutting with low feeds. The low value of feed chosen for these experiments, 0.15 mm/rev, was the lowest that could be used reliably without part failure. Two types of tungsten carbide cutting tools were used: one with a zero

degree rake angle, and another with a positive five degree rake angle. Previous studies with green machining recommend using polycrystalline diamond (PCD) coated inserts because of the high tool wear from cutting an abrasive material [16]. However, PCD tools are not readily available with different rake angles, so tungsten carbide was used instead. The two types of cellulose binders and the two sizes of alumina particles were chosen based on the experience of engineers at Corning Inc. to produce machinable green parts.

Table 4 - Factor levels for experimental design

	Cellulose	**Particle Size**	**Feed (mm/rev)**	**Cutting Speed (m/min)**	**Rake Angle (degrees)**
Low Value	MC	Coarse	0.15	15	0
High Value	HMC	Fine	0.25	75	+5

3.3 Results and Analysis

3.3.1 Cutting Forces

Summary statistics for the resultant force and surface roughness are reported in Table 5. Mean and standard deviation were calculated over the five repetitions for each treatment combination.

Table 5 - Summary statistics for cutting force and surface roughness.

Treatment	Feed	Cutting Speed	Rake Angle	Cellulose	Particle Size	Resultant Force (N)		Roughness, Sa (µm)	
						Mean	St. Dev	Mean	St. Dev
1	-	-	-	-	+	94.93	5.24	3.35	0.43
2	-	-	-	+	-	71.75	5.8	2.89	0.45
3	-	-	+	-	-	84.29	5.67	2.19	0.1
4	-	-	+	+	+	79.56	6.12	2.1	0.15
5	-	+	-	-	-	43.6	4.93	2.58	0.37
6	-	+	-	+	+	59.26	10.86	2.92	0.46
7	-	+	+	-	+	70.69	14.54	2.01	0.14
8	-	+	+	+	-	55.5	3.6	2.21	0.11
9	+	-	-	-	-	30.68	2.92	6.37	0.74
10	+	-	-	+	+	36.94	9.99	6.12	0.87
11	+	-	+	-	+	59.78	2.88	3.61	0.46
12	+	-	+	+	-	41.75	6.57	2.76	0.26
13	+	+	-	-	+	45.52	10.94	6.29	0.69
14	+	+	-	+	-	25.78	14.91	4.95	0.36
15	+	+	+	-	-	49.38	3.65	3.44	0.33
16	+	+	+	+	+	70.21	7.98	3.69	0.37

An analysis of variance (ANOVA) was performed for the effect of the treatment factors on resultant cutting force. The results are shown in Table 6. The probability for rejecting the null hypothesis, or alpha, was set at 5% as a minimum cutoff for determining statistical significance. Main effect plots and interaction effect plots for the statistically significant factors are shown below.

Table 6 - ANOVA with resultant force (N) as the dependent variable.

	DF	Sum of Squares	Mean Square Error	F-Value	P-Value	Significance
Cellulose	1	88.25	88.25	0.72	0.401	
Particle Size	1	17338.31	17338.31	140.49	0.000	***
Feed	1	3818.96	3818.96	30.94	0.000	***
Speed	1	906.09	906.09	7.34	0.009	**
Rake	1	7783.95	7783.95	63.07	0.000	***
Cellulose*Particle Size	1	2170.88	2170.88	17.59	0.000	***
Cellulose*Feed	1	1008.65	1008.65	8.17	0.006	**
Cellulose*Speed	1	139.26	139.26	1.13	0.292	
Cellulose*Rake	1	607.48	607.48	4.92	0.030	*
Particle Size*Feed	1	1.72	1.72	0.01	0.906	
Particle Size*Speed	1	10.17	10.17	0.08	0.775	
Particle Size*Rake	1	353.84	353.84	2.87	0.095	
Feed*Speed	1	267.63	267.63	2.17	0.146	
Feed*Rake	1	405.88	405.88	3.29	0.074	
Speed*Rake	1	108.63	108.63	0.88	0.352	
Residuals	64	7898.5	123.41			
Total	79	42908.18				
Significance was tested at 5% with the following abbreviations: *=0.05, **=0.01, ***=0.001						

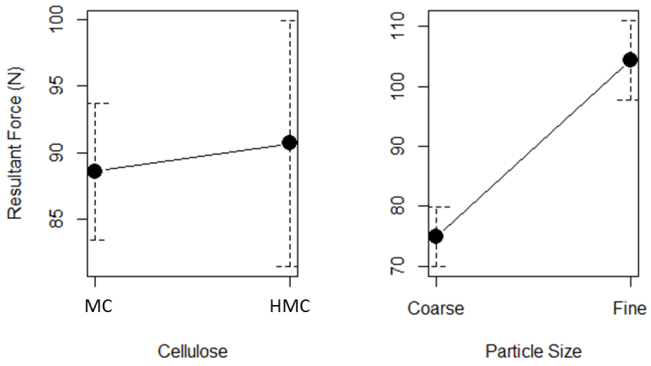

Figure 6 - Main effect plots for cellulose and particle size on resultant force.

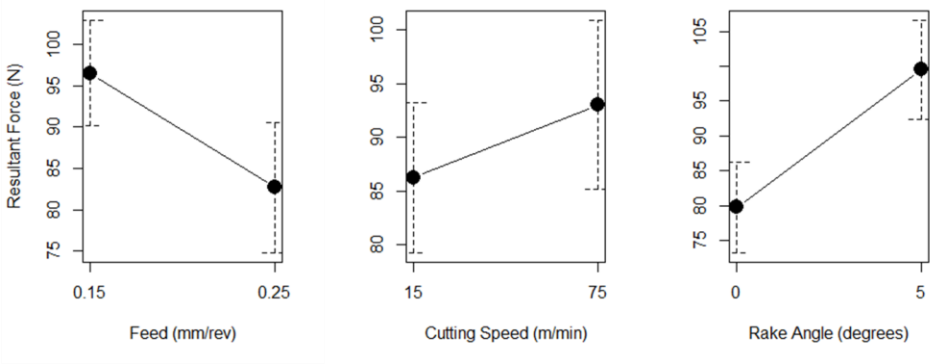

Figure 7 - Main effect plots for feeds, cutting speed, and rake angle on resultant force.

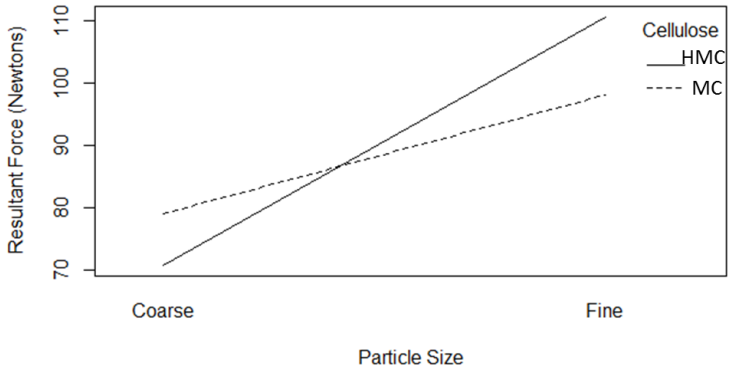

Figure 8 - Interaction effect for particle size and cellulose on resultant force.

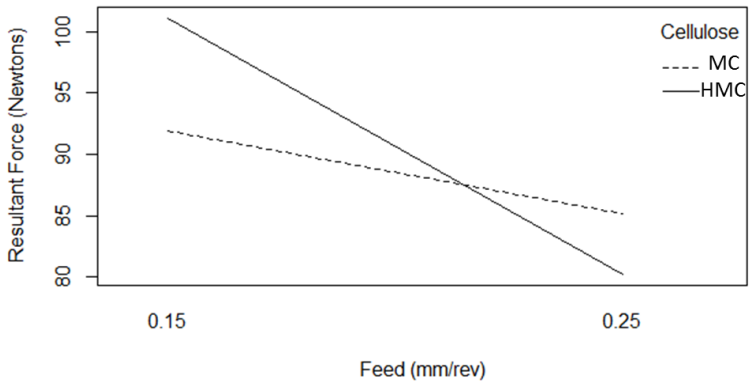

Figure 9 - Interaction effect plot for cellulose and feed on resultant force.

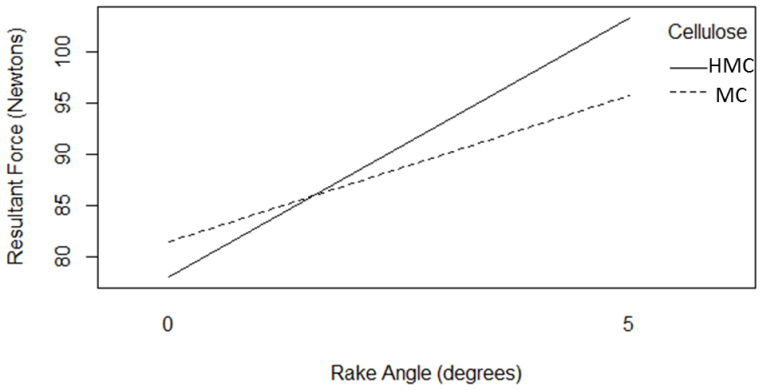

Figure 10 - Interaction effect plot for cellulose and rake angle on resultant force.

Table 6 shows that all the main factors except cellulose were statistically significant in their correlation with resultant force. Cellulose had significant second order interactions with particle size, feed, and rake angle, despite cellulose not having a significant main effect. Figure 6 and Figure 7 show that higher forces occurred for alumina rods with finer particle size, lower feed, higher cutting speed, and positive rake angle. Additionally, those plots show that particle size, feed, and rake angle had the largest effect on force for the range of levels examined. The interaction plots also show that the effect of particle size, feed, and rake angle were all amplified for samples with HMC binder instead of MC.

The impact of feed on cutting force is surprising because other green machining studies have noted higher forces at greater feeds, while the opposite was observed here [7, 10, 11]. In the study on micro-milling green ceramics [11], however, it was noted that increasing feed for a workpiece with wax removed from the binder led to lower forces. The authors argued that for this particular green ceramic, the drop in force was due to a transition from ploughing to cutting. During the preliminary cutting tests, green samples would often spontaneously rupture, especially at feeds below the 0.15 mm/rev used in these experiments. It's possible that ploughing still occurred, even at these higher feeds, which would explain why forces dropped as feed increased.

Machining of other brittle materials have shown that brittle fracture modes involve cracks propagating ahead of the cutting zone, leading to the chips breaking off [19]. It has been shown that a higher feed causes a transition from ductile to brittle machining, with the latter characterized by the brittle fracture mode and higher forces. However, all of the longitudinal cutting of green alumina in the current study produced powder instead of solid chips, meaning that only brittle machining occurred at all feeds. Another surprising result is that the positive rake angle tool produced higher forces. Studies of machining brittle materials show that more negative rake angles normally result in higher forces due to higher friction and hydrostatic pressure [20]. Further work is needed to obtain a physical explanation for this result.

Other studies have also examined the effect of cutting speed on forces, and they noted either no effect [7] or a small increase in force with an increase in speed [10]. This matches the results in Figure 7, which shows a positive correlation that is much smaller than the effect of particle size, feed, and rake. Another study noted an interaction effect

between cutting speed and feed at higher feeds [11]. However, the results of this study didn't find that interaction to be statistically significant.

3.3.2 Surface Roughness

Another ANOVA was performed for the effect of the treatment factors on surface roughness. Main effect plots and interaction effect plots for the statistically significant factors are shown below.

Table 7 - ANOVA with surface roughness (Sa, µm) as the dependent variable.

	DF	Sum of Squares	Mean Square Error	F-Value	P-Value	Significance
Cellulose	1	1.53	1.53	7.56	0.008	**
Particle Size	1	2.27	2.27	11.24	0.001	**
Feed	1	90.2	90.2	446.3	0.000	***
Speed	1	0.52	0.52	2.59	0.112	
Rake	1	56.66	56.66	280.36	0.000	***
Cellulose*Particle Size	1	0.55	0.55	2.71	0.105	
Cellulose*Feed	1	1.5	1.5	7.42	0.008	**
Cellulose*Speed	1	0.39	0.39	1.93	0.170	
Cellulose*Rake	1	0.47	0.47	2.32	0.132	
Particle Size*Feed	1	0.86	0.86	4.28	0.043	*
Particle Size*Speed	1	0.18	0.18	0.9	0.347	
Particle Size*Rake	1	0.38	0.38	1.87	0.176	
Feed*Speed	1	0.03	0.03	0.16	0.695	
Feed*Rake	1	15.34	15.34	75.89	0.000	***
Speed*Rake	1	2.25	2.25	11.15	0.001	**
Residuals	64	12.94	0.2			
Total	79	186.08				
Significance was tested at 5% with the following abbreviations: *=0.05, **=0.01, ***=0.001						

For the effect on surface roughness, all the main effects except cutting speed were statistically significant. Additionally, the second level interactions for feed with cellulose, particle size, and rake angle were all significant, as well as the interaction of rake angle and cutting speed. Figure 11 and Figure 12 show that surface roughness was higher for MC binder, fine particle size, high feed, and zero degree rake angle. Figure 13, Figure 14, and Figure 15 show that the effect of feed on roughness was amplified for MC, fine particle size, and zero degree rake angle. Lastly, Figure 16 shows that rake angle has a larger effect at low cutting speeds. Overall, the data shows that feed and rake angle have the largest effect on surface roughness. This agrees with other studies that found higher feed increased roughness and that cutting speed had no effect [7, 10].

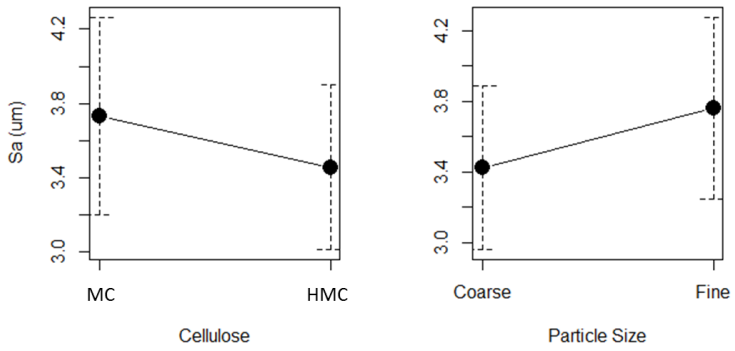

Figure 11 - Main effect plots for cellulose and particle size on surface roughness (Sa).

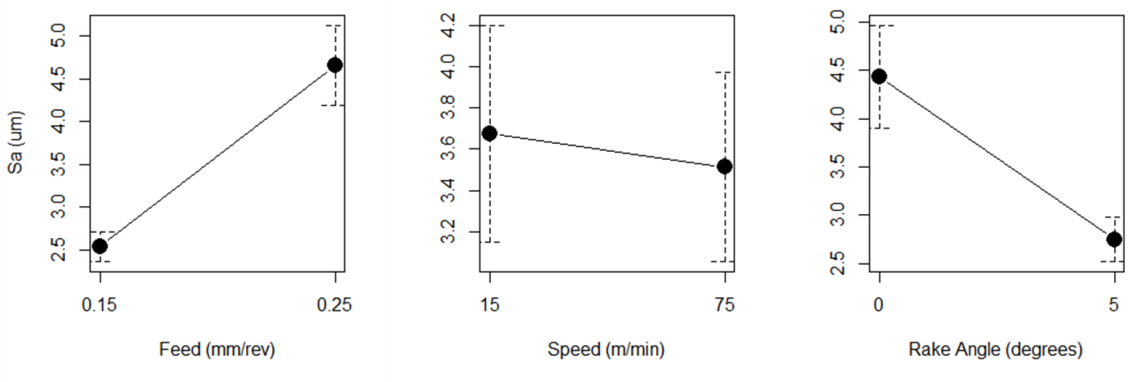

Figure 12 - Main effect plots for feed, cutting speed, and rake angle on surface roughness (Sa).

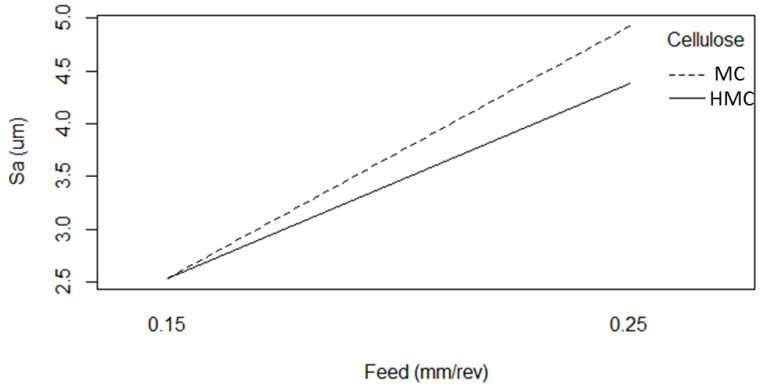

Figure 13 - Interaction effect plot of cellulose and feed on surface roughness (Sa).

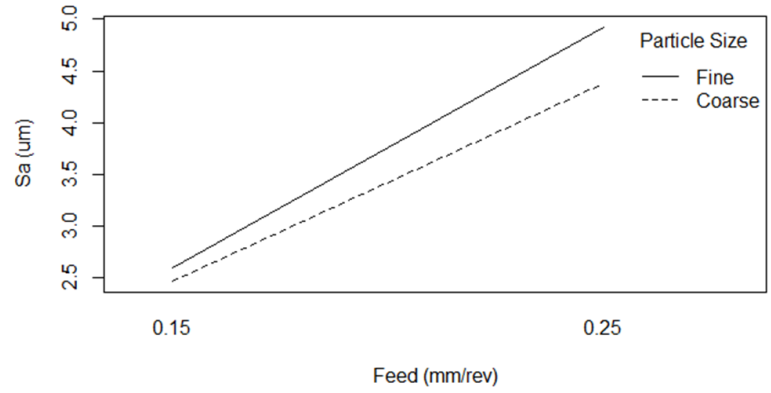

Figure 14 - Interaction effect plot of particle size and feed on surface roughness (Sa).

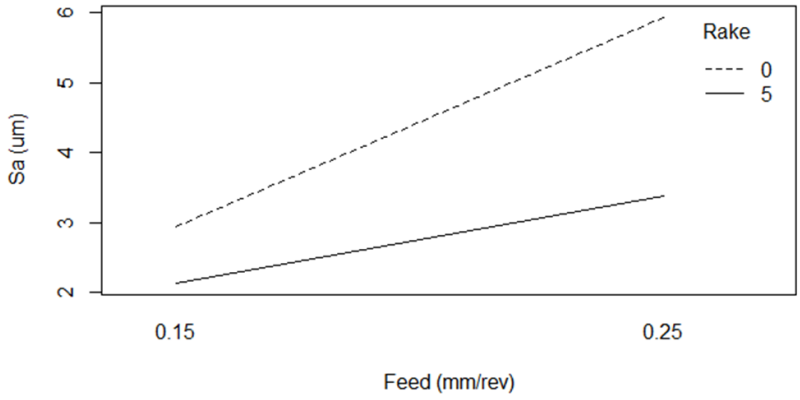

Figure 15 - Interaction effect plot of rake angle and feed on surface roughness (Sa).

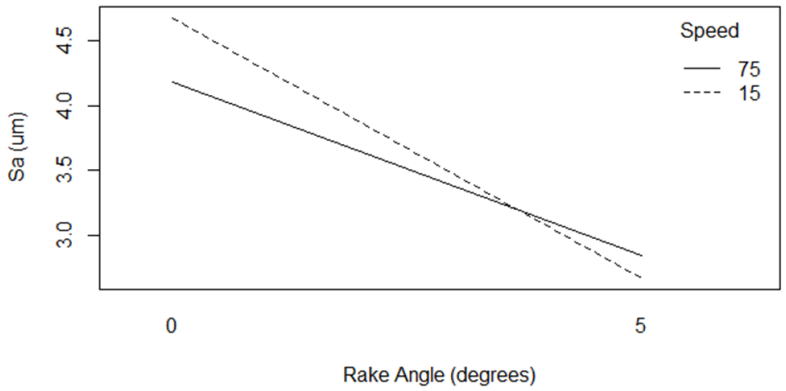

Figure 16 - Interaction effect plot of rake angle and cutting speed on surface roughness (Sa).

3.3.3 Imaging

Figure 17 shows three-dimensional images from the ZeGage white light interferometer of the surfaces of four machined samples, organized by cutting speed and feed. All four are for samples made with MC binder and machined with the zero degree rake angle tool. The letters ‘C’ and ‘F’ on each image refer to coarse and fine particle size, respectively. Figures for cutting tests for other rake angle and cellulose combinations are in Appendix A. Individual granules of alumina and binder are clearly visible for samples with a coarse particle size. In addition, the feed lines are visible in all cases, with the lines more spread out and larger in height for samples cut with higher feeds, as expected. The roughness is also visibly higher for zero degree rake angle tests compared to the same levels of the other factors. This matches the results of the statistical analysis.

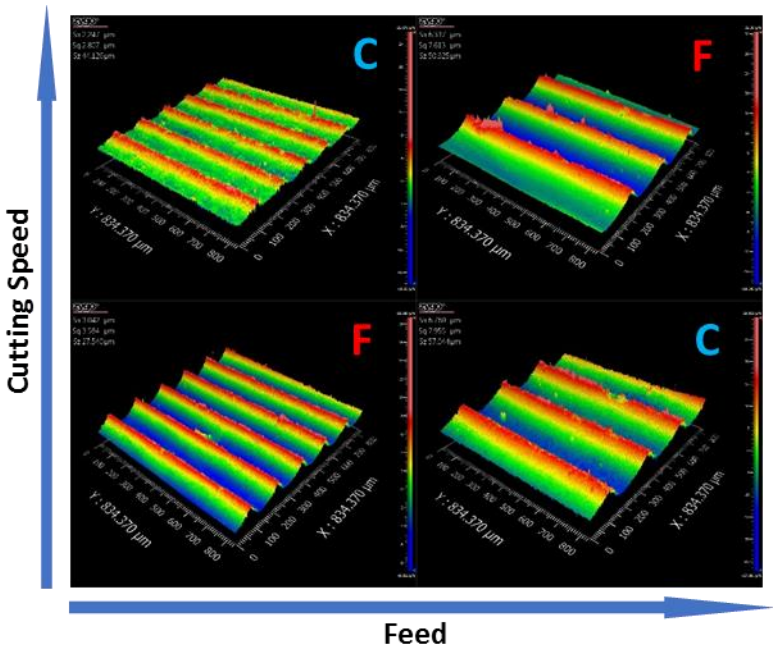

Figure 17 - Interferometer images of samples machined with 0 degree rake angle tool and MC binder.

Figure 18 has optical images of surfaces of samples with MC binder that were machined using the zero degree rake angle tool. The same organization as in Figure 17 is used, and figures for the other rake angle and binder combinations are in Appendix A as well. The coarser particles are clearly visible, whereas the fine particle size images appear to be much smoother. Small voids are visible in the machined surfaces, especially for samples with the fine particle size. However, the feed marks are the largest features on the surfaces. This agrees with the results of the ANOVA analysis, which showed that feed was the greatest determinant of surface roughness. Surface cracks occurred occasionally, but were not common.

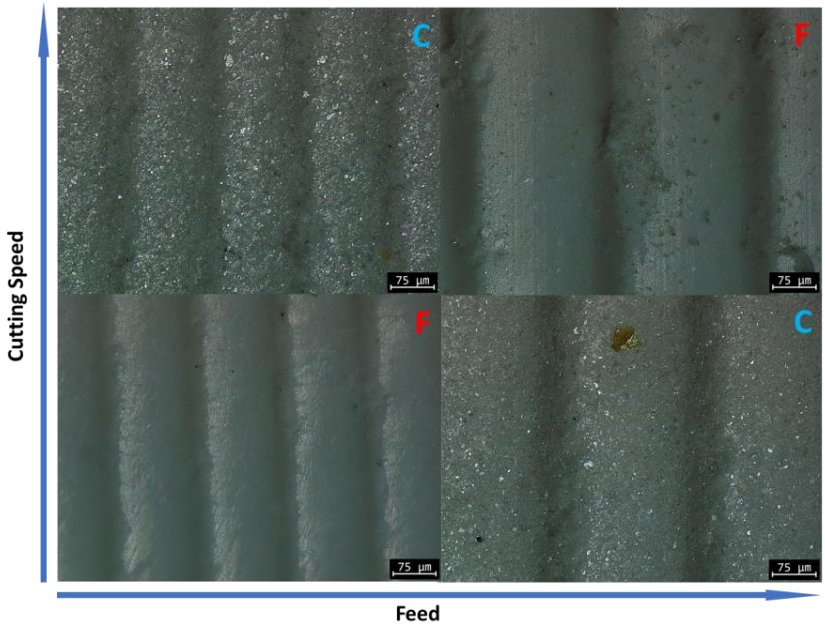

Figure 18 - Optical images of samples machined with 0 degree rake angle tool and MC binder.

3.4 Summary

Longitudinal turning experiments were performed with small sections of green alumina rods to determine the effect of cutting parameters and green ceramic composition on cutting forces and surface roughness. Analysis showed that many of the factors were statistically significant. In particular, feed, particle size, and rake angle were all shown to have large effects on cutting force, while feed and rake angle had large effects on surface roughness. Surprisingly, higher feed was found to decrease cutting force, which may be due to relatively more ploughing occurring at low feeds. Additionally, the positive rake angle tool had higher machining forces than the zero degree take tool.

CHAPTER 4. BENDING STRENGTH

4.1 Introduction

Surface and subsurface damage has been shown to reduce strength after machining of ceramics in the fired state [2]. It is unknown if similar mechanisms are responsible for reductions in bending strength after green machining. Studies on the effect of surface roughness after green machining on bending strength in the green and fired state have shown that strength sometimes increased or decreased as roughness increased [7, 8, 13].

In the previous chapter, experiments were used to determine how machining process parameters and material characteristics of the green ceramic impact the cutting forces and surface roughness. It is unknown if cutting forces correlate with machining induced damage in green ceramics, and surface roughness may be the strength determining factor if it is the largest flaw on the surface. In this chapter, the effect of cutting forces and surface roughness on the strength of green machined ceramics was explored using four-point bending tests of unfired alumina rods.

Three factors were varied during machining of the rods according to an experimental design such that the rods would have different cutting forces and surface roughness. Statistical analysis was used to correlate the force and roughness with the bending strength.

4.2 Experimental Procedure

4.2.1 Rod Preparation and Testing

The ASTM C1684 standard for flexure tests of cylindrical ceramic samples was used as a guide for the four-point bend tests [17]. The standard gives recommended and allowable sizes for the rods depending on the length of the support spans. A large enough length to diameter ratio is necessary to avoid failure from contact cracks at the lower supports during four-point bend test, which would invalidate the test. The span for the lower supports used in these tests, 20 mm, requires the rods to be at least 25 mm long and at most 6.7 mm diameter. Instead, the alumina rods were machined to 25.4 mm (1”) length and 7.62 mm (0.3”) diameter, which is long enough but too thick. However, attempts to machine rods of greater length or smaller diameter resulted in the spontaneous fracture of the specimens, so the current rod size was used instead.

The procedure for machining and data collection was similar to that described in Chapter 3. Sample preparation was performed using longitudinal turning of as-extruded green alumina rods on the CNC lathe, forces were measured during the cutting test with the three-component piezoelectric force dynamometer (Kistler 9256C2), and then the machined sections were removed from the rest of the green alumina rods using the diamond wire saw (Murg 24-A) so that the roughness of the machined surface could be measured with the white light scanning interferometer (Zygo Zegage Pro). The same tungsten carbide inserts used in Chapter 3 were used here.

As before, the extruded alumina samples needed to be turned under gentle conditions to achieve circular rods before the final cutting test. This was done until the rods

reached 12.7 mm (0.5”) diameter. Tests were performed using 2.54 mm (0.1”) radial depth of cut, such that the final diameter of the machined rods was 7.62 mm (0.3”). The feed, rake angle of the tool, and the type of binder used to cut each rod was determined based on the testing matrix given in the next section.

Four-point bend tests were performed using an Instron 5982 Universal Testing System with a semi-articulating fixture for the top support. Configuration A from ASTM C1684 was used, which specifies a 10 mm span for the upper supports and a 20 mm span for the lower supports [17]. A diagram of the four-point bend setup is shown in Figure 19. Gasket material was adhered between the lower supports and the sample to prevent contact cracks from forming that would lead to an invalid test failure. Samples were loaded at a rate of 1 mm/min until failure, when a 50% drop in force occurred. In all tests, the samples failed when the sample fractured in two. Optical images were taken of the fractured surfaces to observe how failure occurred.

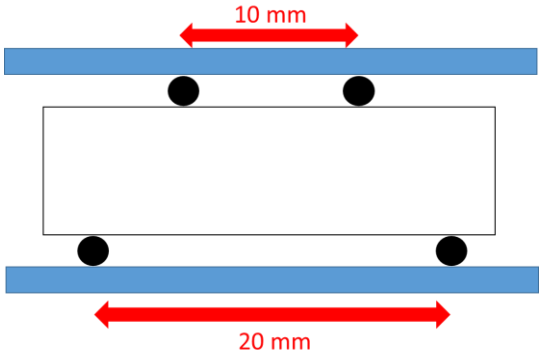

Figure 19 - Diagram of the four-point bend setup.

4.2.2 Experimental Design

The experimental design for the bending experiments is similar to the one used in Chapter 3, with some factors removed. The new design uses a 2^3 full factorial with ten repetitions each, for 80 total data points. Factors were chosen for inclusion based on whether they were found to have had a strong impact on cutting forces and surface roughness in the previous cutting experiment. Feed and rake angle were included because they had large and statistically significant effects on both, and cellulose was included because it had significant second order interactions with feed and rake angle.

Particle size was found to be significant as well, but it needed to be excluded because machined alumina rods with fine particle size could not be produced. During initial attempts at machining 25.4 mm (1”) long rods, samples made from the fine particle size alumina powder failed spontaneously. Lastly, cutting speed was excluded because it had a very minor effect on both force and roughness. Table 8 shows the test matrix and Table 9 shows the levels for each factor. The high and low levels of the factors are the same as for the last experiment, seen in Table 4, except only coarse particle size and 50 m/min cutting speed were used for all tests.

Table 8 - Experimental test matrix for flexure tests.

Treatment	Feed	Rake Angle	Cellulose
1	-	-	-
2	-	-	+
3	-	+	-
4	-	+	+
5	+	-	-
6	+	-	+
7	+	+	-
8	+	+	+

Table 9 - Factor levels for bending strength experiment.

	Cellulose	Particle Size	Feed (mm/rev)	Cutting Speed (m/min)	Rake Angle (degrees)
Low Value	MC	Coarse	0.15	50	0
High Value	HMC		0.25		5

4.3 Results and Analysis

4.3.1 Flexure Strength

Table 10 gives the summary statistics for the flexure strength, as well as Weibull statistics for each treatment combination. Weibull distributions are used for the strength of ceramics because brittle materials fail from their largest flaw. The two-parameter Weibull distribution is characterized by the characteristic strength ($\boldsymbol{\sigma_0}$) and shape parameter (m), also known as the modulus. The first gives the strength at which 63.2% samples will have failed. The second describes the shape of the statistical distribution, with a higher value denoting a more symmetric distribution with a smaller width [18].

Note that 30 tests minimum are recommended for using a Weibull distribution for the strength of ceramics, and at most ten were used here. A sample size of ten was chosen

because preparing green ceramic rods, machining then, and performing four-point bend tests is highly time consuming. Additionally, ten samples per analysis is common in other studies with green ceramics [7, 8].

No trends are apparent in the mean strength, because any difference in strength between treatments is masked by the large standard deviation of each test. The characteristic strength and shape parameter of the Weibull statistics also do not show any consistent trends.

Table 10 - Summary and Weibull statistics for flexure strength.

Treatment	Feed	Rake Angle	Cellulose	Flexure Strength (MPa)		Weibull		
				Mean	St. Dev.	σ_0 (MPa)	m	Sample Size
1	-	-	-	15.95	1.89	16.76	9.75	9
2	-	-	+	15.17	1.34	15.78	12.77	8
3	-	+	-	16.09	1.19	16.64	15.31	10
4	-	+	+	15.94	1.83	16.73	10.03	9
5	+	-	-	15.77	1.35	16.36	13.69	9
6	+	-	+	15.22	1.98	16.05	9.03	9
7	+	+	-	15.17	1.50	15.83	11.65	9
8	+	+	+	15.79	1.74	16.54	10.59	10

Table 11 shows the results of an ANOVA for the effect of resultant cutting force and surface roughness (Sa) on flexure strength. The probability for rejecting the null hypothesis, or alpha, was set at 5% as a minimum cutoff for determining statistical significance. Neither factor was found to have a statistically significant effect on the green strength of the machined alumina at any level. Other studies have also shown that green machining did not significantly change the characteristic strength, but that the modulus was effected [7, 13]. Some found that green machining reduced strength when samples were

tested in the fired state and that the strength reduction correlated with rougher surface. However, this doesn't appear to be the case when testing is performed in the green state [7, 8]. Overall, the results show that the cutting forces and surface roughness in green machining did not significantly impact the green strength. Whether this conclusion extends to the fired strength is unknown.

Table 11 - ANOVA for the effect of cutting force and surface roughness on bending strength.

	DF	Sum of Squares	Mean Square Error	F-Value	P-Value	Significance
Surface Roughness	1	1.46	1.46	0.57	0.454	
Resultant Force	1	0.18	0.18	0.07	0.791	
Residuals	70	179.82	2.57			
Total	72	181.46				
Significance was tested at 5% with the following abbreviations: *=0.05, **=0.01, ***=0.001						

4.3.2 Fractured Surfaces

Figure 20 shows the fractured surfaces of four alumina rods made with coarse alumina particles and MC binder that were then broken in four-point bend tests. They are organized from low to high by rake angle and feed on the vertical and horizontal axes, respectively. Another series of images for samples with HMC binder are shown in Figure 21 .Failure during testing begins at the bottom of each image, where tensile load is applied during 4-point bending. Many pores are visible in the images, but failure doesn't appear to originate from them.

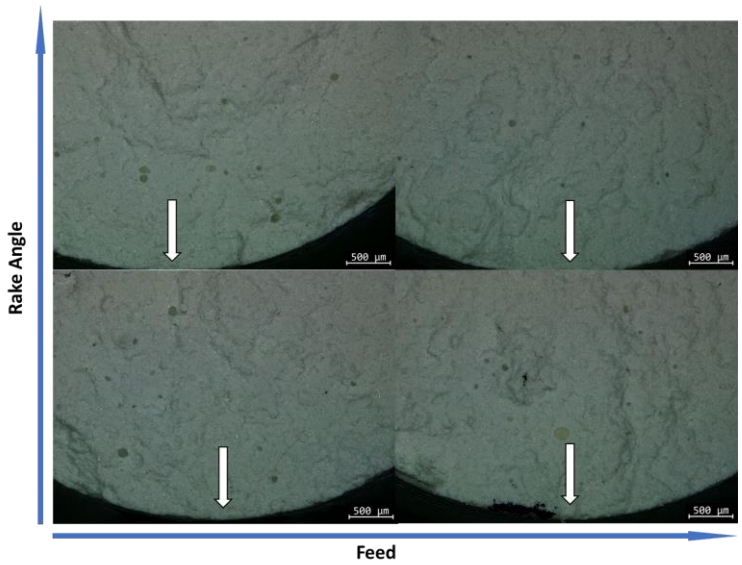

Figure 20 - Cracked surfaces of alumina rods made with MC binder and coarse particle size. White arrows mark the bottom surface where failure initiated. Axes show the levels of feed and rake for each image.

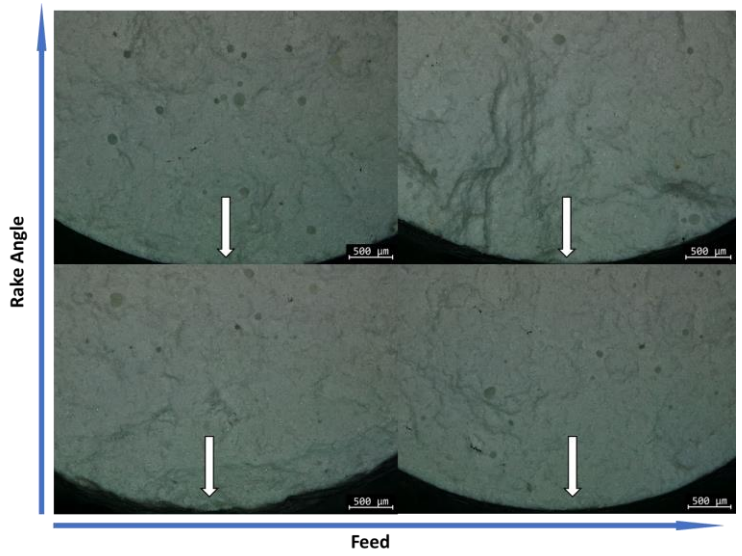

Figure 21 - Cracked surfaces of alumina rods made with HMC binder and coarse particle size. White arrows mark the bottom surface where failure initiated. Axes show the levels of feed and rake for each image.

Cracks were also observed near the surface and in the bulk of some samples. However, failure did not appear to originate from these cracks. Figure 22 shows a close-up image of one such crack.

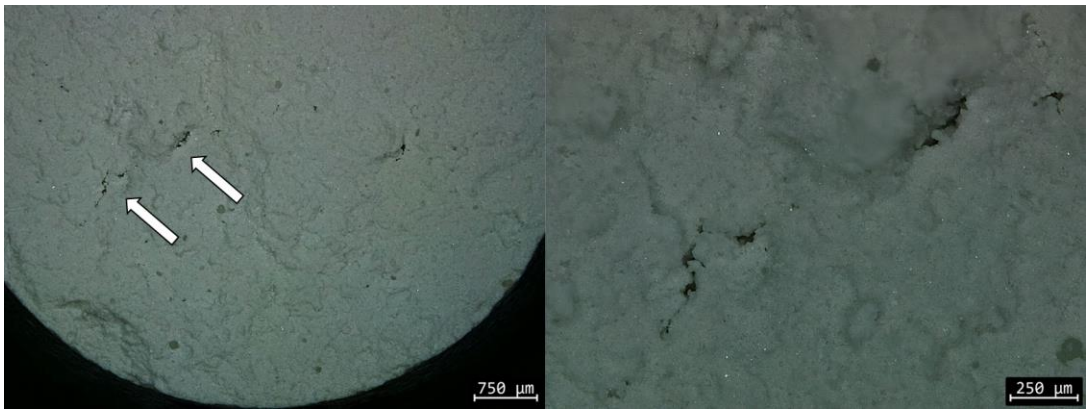

Figure 22 - Cracked surface of an alumina rod. Rod was produced with MC binder and coarse particle size. Machining was performed with 0.15 mm/rev feed and zero degree rake angle. Right image is zoom in of cracks that are marked with arrows in the left picture.

4.4 Summary

Bending tests were performed to determine the strength of green alumina rods machined under various conditions. These conditions were chosen to create samples of varying cutting force and surface roughness so that these measurements could be correlated to bending strength. However, statistical analysis did not find any significant effect for either cutting force or surface roughness on strength in the green state.

One explanation for these results is that machining did not induce subsurface or surface damage, or that the change in strength was smaller than the inherent variability of the green alumina's strength. Alternatively, machining may have induced damage, but the damage is smaller than the flaws created during extrusion. Optical images of the cracked

surfaces showed cracks and pores, but none appeared to be to be origins for failure during the bending tests. Lastly, machining induced damage might not be as important for the strength of green ceramics as they are for fired ceramics due the extra ductility provided by the polymer binder. However, any flaws, either from machining or extrusion, may persist after firing where they could impact the strength of the fired part. Further study is necessary to understand how green machining impacts the fired strength.

CHAPTER 5. CONCLUSION

5.1 Summary

Two sets of longitudinal turning experiments were performed with green alumina to determine how process parameters during green machining and material composition of the extruded green part impact the quality of the green part, and how the green strength might be impacted by machining.

The cutting experiment found that many factors were statistically significant for their relationship with resultant force and surface roughness. In particular, the feed, rake angle, and particle size were all important for force. High feed, zero-degree rake, and coarse particle size all reduced the magnitude of the resultant force. For surface roughness, feed and rake angle were the most important factors. The smoothest surface was achieved with low feed and positive rake angle. Cellulose and speed were often significant as were some of their interactions, but both had a much smaller effect on force and roughness than did the other factors.

The negative correlation between feed and cutting force was unexpected. Low feeds may have caused more ploughing than cutting, which would cause higher forces than in the high feed condition where cutting dominated. The positive five degree rake tool also had higher forces, which contradicts findings in other brittle machining studies. Additionally, the low surface roughness achieved with positive rake angle was surprising as one study had predicted more surface cracks with positive rake angles [15]. However,

optical and interferometer images of the surfaces showed few cracks, and feed lines were the largest surface feature.

The results of the flexure tests found no correlation between either resultant force or surface roughness with bending strength of green machined rods tested in the green state. The inherent variability of the green strength regardless of machining was larger than any changes in strength from machining. This agrees with other studies on machined green strength [7, 13]. Images of the fractured surface only showed pores and small cracks, but no obvious flaws from machining.

5.2 Future Work

Future work is needed to determine whether green machining impacts strength of fired ceramics, and if so then what particular mechanism determines the reduction, whether surface roughness or subsurface cracks. Once this is understood, then process parameters for green machining and the material characteristics of the green body can be chosen before manufacturing to achieve sintered parts with high enough strength for their required applications.

APPENDIX A. OPTICAL IMAGES

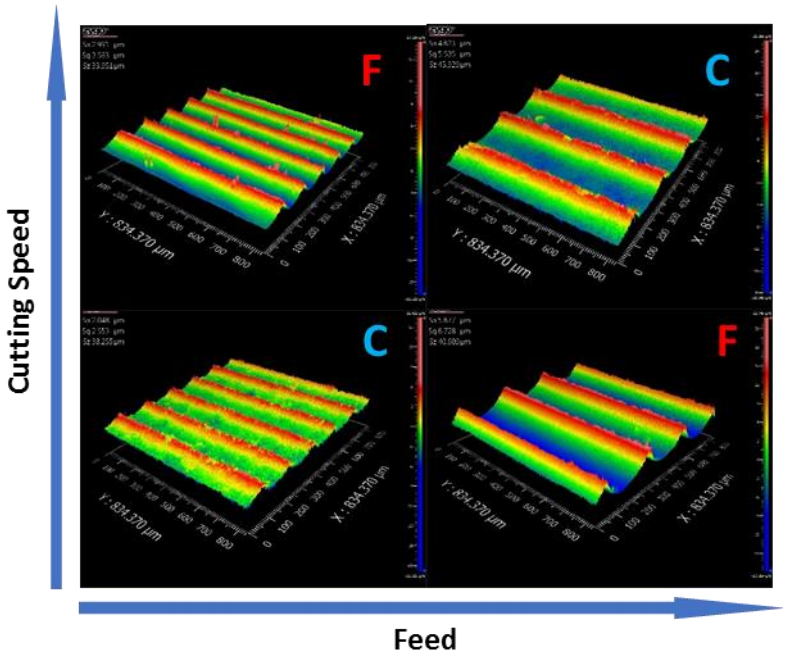

Figure 23 - Interferometer images of samples machined with 0 degree rake angle tool and HMC binder.

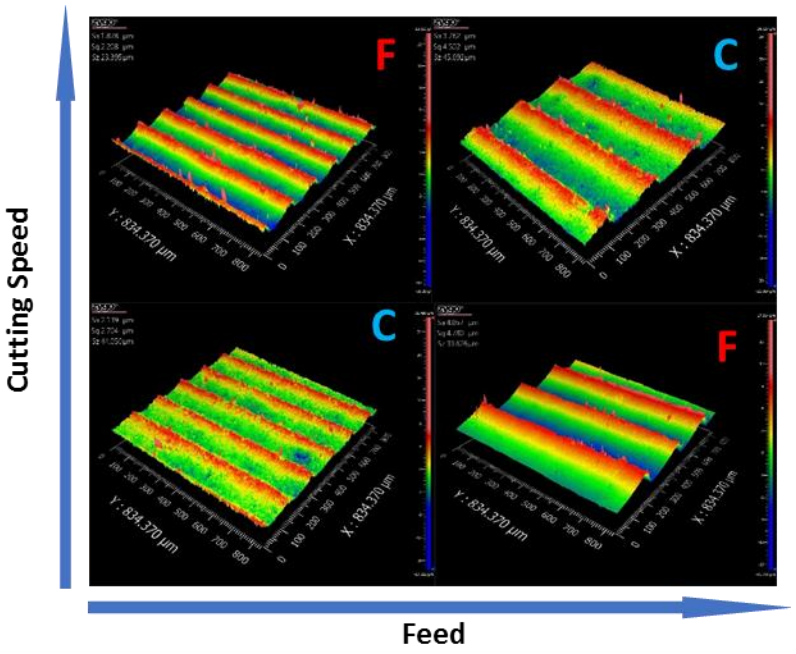

Figure 24 - Interferometer images of samples machined with +5 degree rake angle tool and MC binder.

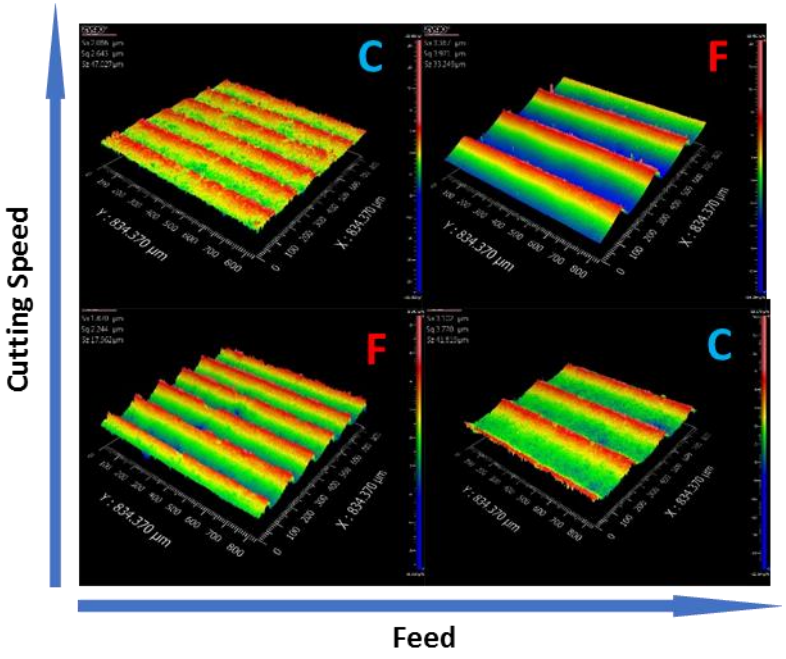

Figure 25 - Interferometer images of samples machined with +5 degree rake angle tool and HMC binder.

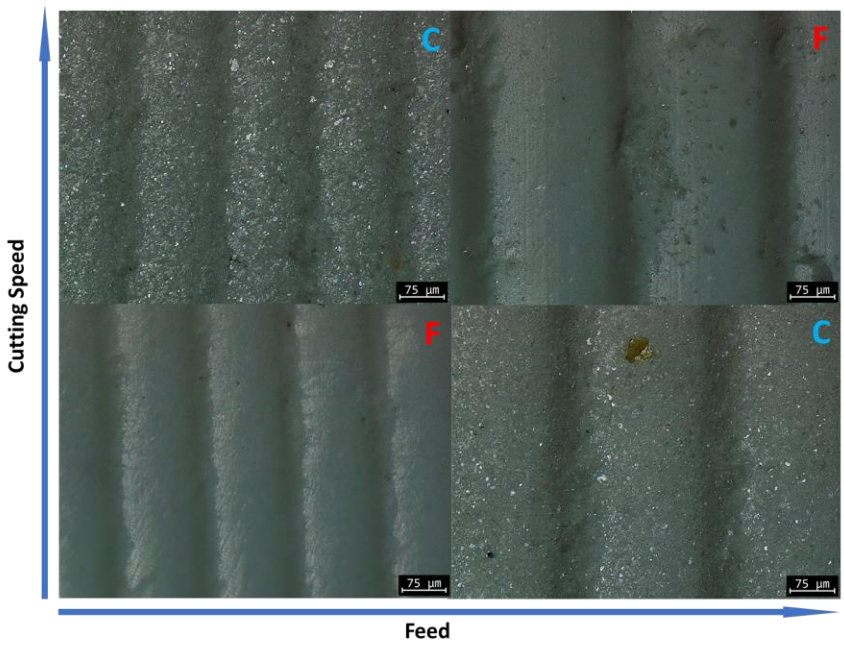

Figure 26 - Optical images of samples machined with 0 degree rake angle tool and HMC binder.

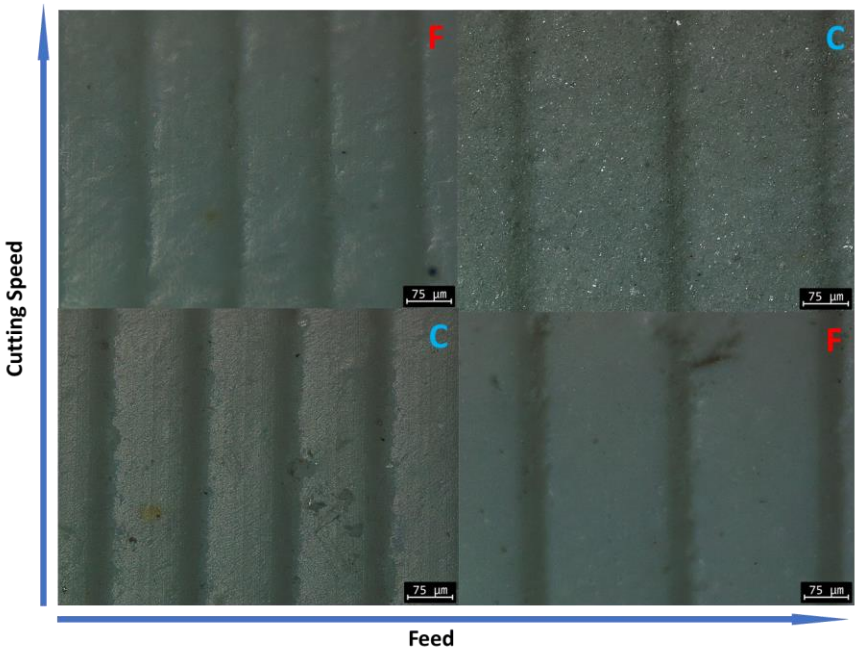

Figure 27 - Optical images of samples machined with +5 degree rake angle tool and MC binder.

5B

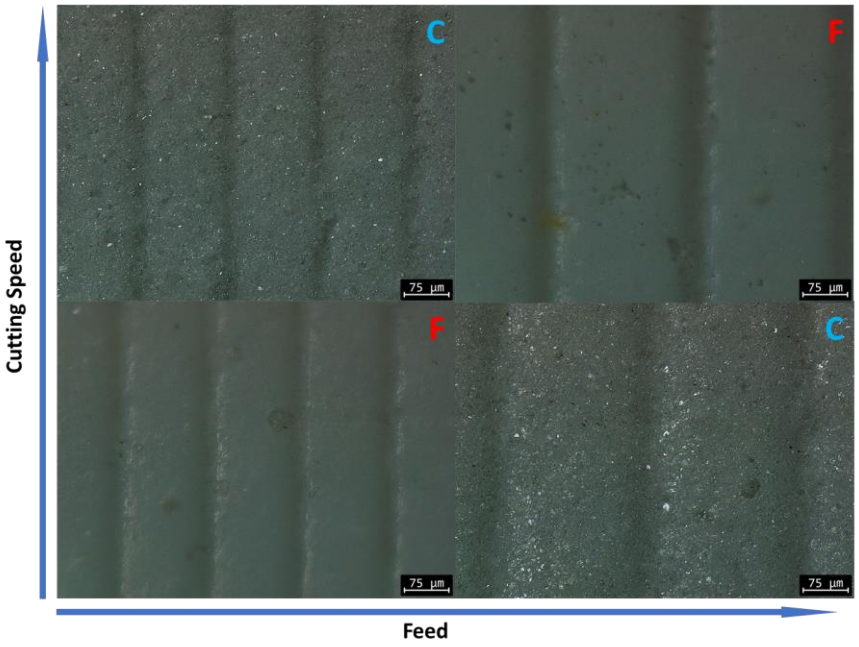

Figure 28 - Optical images of samples machined with +5 degree rake angle tool and HMC binder.

REFERENCES

[1] Kobayashi, Akira. “Precision Machining Methods for Ceramics.” *Advanced Technical Ceramics*, 1989, pp. 261–313., doi:10.1016/b978-0-12-654630-9.50017-6.

[2] Rekow, D, and V P Thompson. “Near-Surface Damage - a Persistent Problem in Crowns Obtained by Computer-Aided Design and Manufacturing.” *Proceedings of the Institution of Mechanical Engineers, Part H: Journal of Engineering in Medicine*, vol. 219, no. 4, 13 Jan. 2005, pp. 233–243., doi:10.1243/095441105x9363.

[3] Thompson, Jeffrey Y., et al. “Ceramics for Restorative Dentistry: Critical Aspects for Fracture and Fatigue Resistance.” *Materials Science and Engineering: C*, vol. 27, no. 3, Apr. 2007, pp. 565–569., doi:10.1016/j.msec.2006.05.034.

[4] Kamboj, R.k, et al. “Machining Behaviour of Green Gelcast Ceramics.” *Journal of the European Ceramic Society*, vol. 23, no. 7, 2003, pp. 1005–1011., doi:10.1016/s0955-2219(02)00265-0.

[5] Desfontaines, M., et al. “Characterisation of the Green Machinability of AlN Powder Compacts.” *Journal of the European Ceramic Society*, vol. 25, no. 6, 2005, pp. 781–791., doi:10.1016/j.jeurceramsoc.2004.03.006.

[6] Ha, Chang-Gi, et al. “Effect of Particle Size on Gelcasting Process and Green Properties in Alumina.” *Materials Science and Engineering: A*, vol. 337, no. 1-2, 3 Jan. 2002, pp. 212–221., doi:10.1016/s0921-5093(02)00034-5.

[7] Maier, H. R., and N. Michaeli. “Green Machining of Alumina.” *Key Engineering Materials*, vol. 132-136, 15 Apr. 1997, pp. 436–439., doi:10.4028/www.scientific.net/kem.132-136.436.

[8] Mohanty, Saralasrita, et al. “Net Shape Forming of Green Alumina via CNC Machining Using Diamond Embedded Tool.” *Ceramics International*, vol. 39, no. 8, 15 May 2013, pp. 8985–8993., doi:10.1016/j.ceramint.2013.04.099.

[9] Nunn, Stephen D., and Glen H. Kirby. “Green Machining of Gelcast Ceramic Materlals.” *Proceedings of the 20th Annual Conference on Composites, Advanced*

Ceramics, Materials, and Structures—A: Ceramic Engineering and Science Proceedings, Volume 17, Issue 3 Ceramic Engineering and Science Proceedings, pp. 209–213., doi:10.1002/9780470314821.ch24.

[10] Onler, Recep, et al. "Forces in Green Micromachining of Aluminum Nitride Ceramics." *Journal of Micro- and Nano-Manufacturing*, 2 Apr. 2019, doi:10.3850/978-981-11-2728-1_79.

[11] Onler, Recep, et al. "Green Micromachining of Ceramics Using Tungsten Carbide Micro-Endmills." *Journal of Materials Processing Technology*, vol. 267, 2019, pp. 268–279., doi:10.1016/j.jmatprotec.2018.12.009.

[12] Su, B., et al. "Green Ceramic Machining: A Top-down Approach for the Rapid Fabrication of Complex-Shaped Ceramics." *Journal of the European Ceramic Society*, vol. 28, no. 11, 15 Apr. 2008, pp. 2109–2115., doi:10.1016/j.jeurceramsoc.2008.02.023.

[13] Westerheide, R., et al. "Advances in Characterisation of Machined Green Compacts." *Journal of the European Ceramic Society*, vol. 17, no. 2-3, 1997, pp. 467–472., doi:10.1016/s0955-2219(96)00174-4.

[14] Bright, E., et al. "Advanced Ceramic Manufacturing of SiALON Exhaust Valves." *SAE Technical Paper Series*, 2 Aug. 1996, doi:10.4271/960051.

[15] El-Wardany, T., et al. "Optimum Process Parameters to Produce Green Ceramic Complex Parts." *CIRP Annals- Manufacturing TEchnology*, vol. 58, no. 1, 2009, pp. 109–112., doi:10.1016/j.cirp.2009.03.105.

[16] Dhara, Santanu, and Bo Su. "Green Machining to Net Shape Alumina Ceramics Prepared Using Different Processing Routes." *International Journal of Applied Ceramic Technology*, vol. 2, no. 3, 2005, pp. 262–270., doi:10.1111/j.1744-7402.2005.02021.x.

[17] ASTM International. *C1684-18 Standard Test Method for Flexural Strength of Advanced Ceramics at Ambient Temperature—Cylindrical Rod Strength*. West Conshohocken, PA, 2018. Web. 12 Apr 2021. https://doi.org/10.1520/C1684-18

[18] ASTM International. *C1239-13(2018) Standard Practice for Reporting Uniaxial Strength Data and Estimating Weibull Distribution Parameters for Advanced*

Ceramics. West Conshohocken, PA, 2018. Web. 12 Apr 2021. https://doi.org/10.1520/C1239-13R18

[19] Qi Liu, Zhirong Liao, Jian Cheng, Dongdong Xu, Mingjun Chen, "Mechanism of chip formation and surface-defects in orthogonal cutting of soft-brittle potassium dihydrogen phosphate crystals." *Materials & Design*, Volume 198, Jan. 2021. https://doi.org/10.1016/j.matdes.2020.109327.

[20] Guo, Xiaoguang, et al. "Study of the Influence of Tool Rake Angle in Ductile Machining of Optical Quartz Glass." *The International Journal of Advanced Manufacturing Technology*, vol. 104, no. 1-4, 2019, pp. 803–813., doi:10.1007/s00170-019-03920-x.